Hypertension Research (2012) 35, 186–193

www.nature.com/hr

ORIGINAL ARTICLE

Cardiac remodeling and diastolic dysfunction in DahlS.Z-*Lepr*^{fa}/*Lepr*^{fa} rats: a new animal model of metabolic syndrome

Tamayo Murase[1], Takuya Hattori[1], Masafumi Ohtake[1], Mayuna Abe[2], Yui Amakusa[2], Miwa Takatsu[1], Toyoaki Murohara[3] and Kohzo Nagata[2]

We recently characterized male DahlS.Z-*Lepr*^{fa}/*Lepr*^{fa} (Dahl salt-sensitive (DS)/obese) rats, which were established from a cross between Dahl salt-sensitive and Zucker rats, as a new animal model of metabolic syndrome (MetS). We have now investigated cardiac pathophysiology and metabolic changes in female DS/obese rats in comparison with homozygous lean female littermates (DahlS.Z-*Lepr*$^{+}$/*Lepr*$^{+}$, or DS/lean, rats). Animals were maintained on a normal diet and were subjected to echocardiography followed by various pathological analyses at 15 weeks of age. Systolic blood pressure was significantly higher in female DS/obese rats than in DS/lean females at 12 weeks of age and thereafter. The survival rate of DS/obese rats was significantly lower than that of DS/lean rats at 15 weeks. Body weight, as well as visceral and subcutaneous fat mass were significantly increased in DS/obese rats, which also manifested left ventricular (LV) diastolic dysfunction and marked LV hypertrophy and fibrosis. In addition, myocardial oxidative stress and inflammation were increased in DS/obese rats compared with DS/lean rats. Serum insulin and triglyceride levels as well as the ratio of low-density lipoprotein- to high-density lipoprotein-cholesterol levels were markedly elevated in DS/obese rats, whereas fasting serum glucose concentrations were similar in the two rat strains. The phenotype of female DS/obese rats is similar to that of MetS in humans. These animals also develop salt-sensitive hypertension and LV diastolic dysfunction as well as LV hypertrophy and fibrosis, and these changes are associated with increased cardiac oxidative stress and inflammation.
Hypertension Research (2012) **35,** 186–193; doi:10.1038/hr.2011.157; published online 15 September 2011

Keywords: cardiac hypertrophy; diastolic dysfunction; metabolic syndrome; myocardial fibrosis; salt-sensitive hypertension

INTRODUCTION

Metabolic syndrome (MetS), a complex of highly debilitating disorders including hypertension, diabetes mellitus and dyslipidemia, is associated with the development of visceral obesity.[1] Adipocytes in visceral fat of obese humans secrete a variety of biological agents that are known as adipocytokines and include proinflammatory cytokines such as tumor necrosis factor (TNF)-α and interleukin (IL)-6 as well as angiotensinogen and leptin.[2] Recent studies have revealed intricate interactions among adipocytes, the sympathetic nervous system and the renin–angiotensin–aldosterone system (RAAS) that contribute to the disturbed metabolic state associated with obesity.[3] Indeed, adipose tissue is thought to have an important role in the development of both hypertension and other complications related to insulin resistance. Activation of the RAAS and associated oxidative stress can result in mitochondrial abnormalities, altered bioenergetics and the accumulation of lipids in the heart, and thereby increase susceptibility to metabolic cardiomyopathy.[4]

Although left ventricular (LV) remodeling and dysfunction have been observed in individuals with MetS,[5,6] the extent of cardiac injury in such individuals has remained unclear. A diet with a moderate fat content was found to induce metabolic abnormalities but did not result in LV diastolic dysfunction in obesity-prone Sprague–Dawley rats.[7] On the other hand, the SHR (spontaneously hypertensive rat)/NDmcr-cp rat, a genetic model of MetS that is a derivative of the SHR with deficiency of the leptin receptor, was shown to develop severe hypertension and LV diastolic dysfunction as well as LV hypertrophy and coronary perivascular fibrosis when fed a high-salt diet.[8] We recently established a new animal model of MetS, the DahlS.Z-*Lepr*^{fa}/*Lepr*^{fa} (Dahl salt-sensitive (DS)/obese) rat, by crossing DS rats and Zucker rats with a missense mutation in the leptin receptor gene (*Lepr*). Male DS/obese rats develop a phenotype similar to MetS in humans, including hypertension, when fed a normal diet. In addition, they develop cardiac hypertrophy as well as renal and liver damage, which may be responsible for their premature death.[9]

[1]Department of Pathophysiology Laboratory Sciences, University Graduate School of Medicine, Nagoya, Japan; [2]Department of Medical Technology, Nagoya University School of Health Sciences, Nagoya, Japan and [3]Department of Cardiology, Nagoya University Graduate School of Medicine, Nagoya, Japan
Correspondence: Professor K Nagata, Department of Medical Technology, Nagoya University School of Health Sciences, 1-1-20 Daikominami, Higashi-ku, Nagoya 461-8673, Japan.
E-mail: nagata@met.nagoya-u.ac.jp
Received 1 June 2011; revised 29 June 2011; accepted 23 July 2011; published online 15 September 2011

These observations suggested that salt sensitivity of blood pressure and target organ damage are enhanced in MetS.

We have now investigated cardiac and systemic pathophysiology, as well as metabolic changes in female DS/obese rats fed a normal diet in comparison with their lean littermates in order to characterize the cardiac phenotype in this animal model of MetS.

METHODS

Animals and experimental protocols

Ten-week-old female inbred DS/obese rats were obtained from Japan SLC (Hamamatsu, Japan) and were handled in accordance with the guidelines of Nagoya University Graduate School of Medicine as well as with the Guide for the Care and Use of Laboratory Animals (US NIH publication no. 85–23, revised 1996). The animals were fed normal laboratory chow containing 0.36% NaCl, and both the diet and tap water were provided ad libitum throughout the experimental period. At 15 weeks of age, rats were placed in metabolic cages for the collection of 24-h urine specimens. They were also anesthetized by i.p. injection of ketamine (50 mg per kilogram of body weight) and xylazine ($10\,mg\,kg^{-1}$), and subjected to echocardiographic analysis. The heart, kidneys and both visceral (retroperitoneal) and subcutaneous (inguinal) fat were subsequently removed and weighed, and LV tissue was separated for analysis. Age-matched female homozygous lean littermates of DS/obese rats (DahlS.Z-*Lepr*$^{+}$/*Lepr*$^{+}$, or DS/lean, rats) served as control animals. Extended details appear in the Supplementary Material online.

Blood pressure measurement and echocardiographic analysis

Systolic blood pressure (SBP) and heart rate were measured weekly in conscious animals by tail-cuff plethysmography (BP-98A; Softron, Tokyo, Japan). At 15 weeks of age, rats were subjected to transthoracic echocardiography, as described previously.[10] In brief, M-mode echocardiography was performed with a 12.5-MHz transducer (Xario SSA-660A; Toshiba Medical Systems, Tochigi, Japan). LV end-diastolic (LVDd) and end-systolic (LVDs) dimensions, and the thickness of the interventricular septum (IVST) and LV posterior wall (LVPWT) were measured, and LV fractional shortening (LVFS), relative wall thickness (RWT) and LV mass were calculated as follows: LVFS (%)=[(LVDd−LVDs)/LVDd]×100; RWT=(IVST+LVPWT)/LVDd; LV mass (g)=({1.04×[(IVST+LVDd+LVPWT)^3−(LVDd)^3]}×0.8)+0.14.[11] LV ejection fraction was calculated with the formula from Teichholz.[12] For assessment of Doppler-derived indices of LV function, both LV inflow and outflow velocity patterns were simultaneously recorded by pulsed-wave Doppler echocardiography. For assessment of LV diastolic function, we calculated the peak flow velocities at the mitral level during rapid filling (*E*) and during atrial contraction (*A*), the *E*/*A* ratio, the deceleration time, and the isovolumic relaxation time (IRT). Both the isovolumic contraction time (ICT) and ejection time (ET) were also determined, and the Tei index, which reflects both LV diastolic and systolic function, was calculated as follows: Tei index=(ICT+IRT)/ET.[13]

Measurement of metabolic and hormonal parameters

Blood was collected from the right carotid artery of rats that had been deprived of food overnight and was centrifuged at 1400 *g* for 10 min at room temperature. The resultant serum and plasma supernatant were kept frozen at –80 °C until analysis. Serum level of glucose was measured by routine enzymatic assays. The concentration of insulin in serum was measured with the use of enzyme-linked immunosorbent assay kits (Morinaga Bioscience Institute, Yokohama, Japan). Plasma renin activity was determined by radioimmunoassay with the use of renin RIA beads (Abbott Japan, Tokyo, Japan). Plasma angiotensin II (Ang II) concentration was determined by radioimmunoassay as described previously,[14,15] and serum aldosterone concentration was measured by radioimmunoassay with the use of a DPC aldosterone kit (Mitsubishi Chemical Medience, Tokyo, Japan). Extended details appear in the Supplementary Material online.

Histology and immunohistochemistry

LV tissue was fixed in ice-cold 4% paraformaldehyde for 48–72 h, embedded in paraffin and processed for histology as described.[16,17] To evaluate macrophage infiltration into the myocardium, we performed immunostaining for the monocyte–macrophage marker CD68 with frozen sections (thickness, 5 μm) that had been fixed with acetone. Endogenous peroxidase activity was blocked by exposure of the sections to methanol containing 0.3% hydrogen peroxide. Sections were incubated at 4 °C first overnight with mouse monoclonal antibodies to CD68 (clone ED1, diluted 1:100; Chemicon, Temecula, CA, USA) and then for 30 min with Histofine Simple Stain Rat MAX PO (Nichirei Biosciences, Tokyo, Japan). Immune complexes were visualized with diaminobenzidine and hydrogen peroxide, and the sections were counterstained with hematoxylin. Image analysis was performed with NIH Scion Image software (Scion Corp., Frederick, MD, USA).

Superoxide production

Nicotinamide adenine dinucleotide phosphate (NADPH)-dependent superoxide production by homogenates prepared from freshly frozen LV tissue was measured with the use of an assay based on lucigenin-enhanced chemiluminescence as described previously.[18] The chemiluminescence signal was sampled every minute for 10 min with a microplate reader (WALLAC 1420 ARVO MX/Light; Perkin Elmer, Waltham, MA, USA), and the respective background counts were subtracted from experimental values. Lucigenin chemiluminescence was expressed as relative light units per mg of protein. Superoxide production in tissue sections was examined by staining with dihydroethidium (Sigma, St Louis, MO, USA) as described.[19] Dihydroethidium is rapidly oxidized by superoxide to yield fluorescent ethidium, and the sections were examined with a fluorescence microscope equipped with a 585-nm long-pass filter. For negative controls, we performed staining with dihydroethidium after incubation of sections with superoxide dismutase ($300\,U\,ml^{-1}$) and confirmed that this procedure abolished the fluorescence (data not shown). The average of dihydroethidium fluorescence intensity values was calculated with the use of NIH Image software (ImageJ).[20]

Quantitative real-time PCR analysis

Total RNA was extracted from LV tissue and treated with DNase with the use of a spin-vacuum isolation kit (Promega, Madison, WI, USA). Complementary DNA was synthesized from 2 μg of total RNA by reverse transcription with random primers (Invitrogen, Carlsbad, CA, USA) and MuLV Reverse Transcriptase (Applied Biosystems, Foster City, CA, USA). Real-time PCR analysis was performed as previously described[21] with a Prism 7000 Sequence Detector (Perkin Elmer) and with primers and TaqMan probes specific for cDNAs encoding atrial natriuretic peptide,[10] brain natriuretic peptide,[10] β-myosin heavy chain,[10] collagen type I,[22] collagen type III,[22] transforming growth factor (TGF)-β1,[10] connective tissue growth factor (CTGF),[18] monocyte chemoattractant protein-1,[18] TNF-α (5′GCTGTACCTTATCTACTCC-3′, 5′-CTGG TATGAAATGGCAAA-3′ and 5′-CTCTTCAAGGGACAAGGCTGC-3′ as the forward primer, reverse primer and TaqMan probe, respectively; GenBank accession no. NM_012675), IL-6 (5′-TTCCCTACTTCACAAGTC-3′, 5′-AGTG GTATATACTGGTCTG-3′ and 5′-AGGAGACTTCACAGAGGATACCAC-3′ as the forward primer, reverse primer and TaqMan probe, respectively; GenBank accession no. NM_012589), angiotensin-converting enzyme,[10] the Ang II type 1A receptor,[10] the mineralocorticoid receptor (MR),[18] serum/glucocorticoid-regulated kinase 1 (5′-AAATCAACCTGGGTCCATCCTC-3′, 5′-ACCTTTCCA AAACTGCCTTTTCC-3′ and 5′-CCCACGCCAAACCCTCTGACTTCCAC-3′ as the forward primer, reverse primer and TaqMan probe, respectively; GenBank accession no. NM_019232), and the $p22^{phox23}$ $gp91^{phox23}$ $p47^{phox}$ (5′-CACCTCTTGAACTTCTTC-3′, 5′-CATTATTCTTGCCATCTTTG-3′ and 5′-ATGTCTCTGGCTTCTTCACCTG-3′ as the forward primer, reverse primer and TaqMan probe, respectively; GenBank accession no. NM_053734), $p67^{phox}$ (5′-TTTGAGGAAGGAGGAGTG-3′, 5′-CGAAGCCAGAAAAATTGT-3′ and 5′-TGAACCACAGAGGCTACAACG-3′ as the forward primer, reverse primer and TaqMan probe, respectively; GenBank accession no. NM_001100984) and Rac1 (5′-CGGTGCTGTCAAATACCTGGA-3′, 5′-TCGGATAGCTTCATCAAA CACTG-3′ and 5′-TCAGCACTCACACAGCGAGGACTCAA-3′ as the forward primer, reverse primer and TaqMan probe, respectively; GenBank accession no. NM_134366) subunits of NADPH oxidase. Reagents for the detection of human 18S rRNA (Applied Biosystems) were used to quantify rat 18S rRNA as an internal standard.

Statistical analysis

Data are presented as means ± s.e.m. Differences between groups of rats at 15 weeks of age were assessed with the Mann–Whitney *U* test. The time courses of body weight, SBP, or heart rate were compared between groups with two-way repeated-measures analysis of variance. Survival rate was analyzed by the standard Kaplan–Meier method and the log-rank test. A *P*-value of <0.05 was considered statistically significant.

RESULTS

LV geometry and function as well as animal survival and metabolic characteristics

Body weight was significantly increased in DS/obese rats compared with DS/lean rats at 11 weeks of age and thereafter (Figure 1a, Table 1). SBP was also significantly higher in DS/obese rats than in DS/lean rats and in female Zucker fatty rats at 11 weeks and thereafter (Figure 1b, Table 1, Figure 1 in Supplementary Material online), whereas heart rate was lower in DS/obese rats during the entire experimental period (Figure 1c, Table 1). SBP tended to be higher in female Zucker fatty rats than in DS/lean rats during the experimental period ($P=0.063$). A total of 7 of 21 (33%) DS/obese rats died during the experimental period (three from renal failure, three from cerebrovascular events and one as a consequence of anesthesia), whereas all DS/lean rats survived. Kaplan–Meier analysis confirmed that the survival rate of DS/obese rats was significantly lower than that of DS/lean rats at 15 weeks (Figure 1d, Table 1). At 15 weeks, the ratios of heart or LV weight to tibial length, indices of cardiac and LV hypertrophy, respectively, were significantly increased in DS/obese rats compared with DS/lean rats, whereas tibial length was significantly shorter in DS/obese rats (Table 1). Uncorrected heart and LV weights were also increased in DS/obese rats (Table 1 in Supplementary Material online). Liver, kidney, visceral and subcutaneous fat weights were increased in DS/obese rats compared with DS/lean rats at 15 weeks. The serum insulin concentration was significantly higher in DS/obese rats than in DS/lean rats, whereas serum glucose levels were similar in the two strains after an overnight fast (Table 1). However, in another group of DS/obese rats ($n=9$), the serum glucose concentration in the non-fasted condition ($472.0 \pm 32.1\,mg\,dl^{-1}$, range of $385.0–710.0\,mg\,dl^{-1}$) was increased markedly compared with that in DS/lean rats ($157.8 \pm 8.9\,mg\,dl^{-1}$, range of $142.0–191.0\,mg\,dl^{-1}$). These data indicate that DS/obese rats develop type 2 diabetes mellitus as well as insulin resistance. The serum leptin concentration in DS/obese rats was ~20 times that in DS/lean rats (Table 2 in Supplementary Material online). Serum levels of total cholesterol, low-density lipoprotein (LDL)-cholesterol, high-density lipoprotein (HDL)-cholesterol and triglyceride, as well as the ratio of LDL-cholesterol to HDL-cholesterol levels were increased in DS/obese rats compared with DS/lean rats. Blood urea nitrogen and urinary protein levels were significantly increased whereas the ratios of creatinine clearance to body or kidney weight were significantly decreased in DS/obese rats compared with DS/lean rats.

Table 1 Anatomic, metabolic and hormonal parameters of DS/lean and DS/obese rats at 15 weeks of age

Parameter	*DS/lean*	*DS/obese*
Body weight (g)	245.2 ± 6.6	385.2 ± 12.0*
Tibial length (mm)	35.1 ± 0.5	33.0 ± 0.2*
SBP (mmHg)	137.2 ± 3.2	176.3 ± 5.8*
Heart rate (beats per min)	435.0 ± 15.0	378.5 ± 13.6*
Heart weight/tibial length ($mg\,mm^{-1}$)	24.5 ± 0.8	36.1 ± 0.5*
LV weight/tibial length ($mg\,mm^{-1}$)	17.8 ± 0.5	26.9 ± 0.5*
Serum glucose ($mg\,dl^{-1}$)	116.2 ± 3.9	120.5 ± 6.4
Serum insulin ($ng\,ml^{-1}$)	0.21 ± 0.08	2.79 ± 0.46*
HOMA–IR	1.8 ± 0.8	22.1 ± 5.2
Plasma renin activity ($ng\,ml^{-1}\,h^{-1}$)	7.36 ± 0.74	1.32 ± 0.28*
Plasma Ang II ($pg\,ml^{-1}$)	25.7 ± 2.1	15.2 ± 2.2*
Serum aldosterone ($pg\,ml^{-1}$)	276.3 ± 22.1	303.4 ± 31.2
Aldosterone/renin ratio	46.0 ± 7.0	273.3 ± 48.2*
Survival (%)	100	67*

Abbreviations: Ang II, angiotensin II; DS, Dahl salt-sensitive; *E/A* ratio, peak flow velocities at the mitral level during rapid filling (*E*) and during atrial contraction (*A*); HOMA–IR, homeostasis model assessment–insulin resistance; LV, left ventricular; SBP, systolic blood pressure.
*$P<0.05$ *vs.* DS/lean rats.
With the exception of survival rate, data are means ± s.e.m. for surviving animals ($n=10$ and 14 for DS/lean and DS/obese rats, respectively).

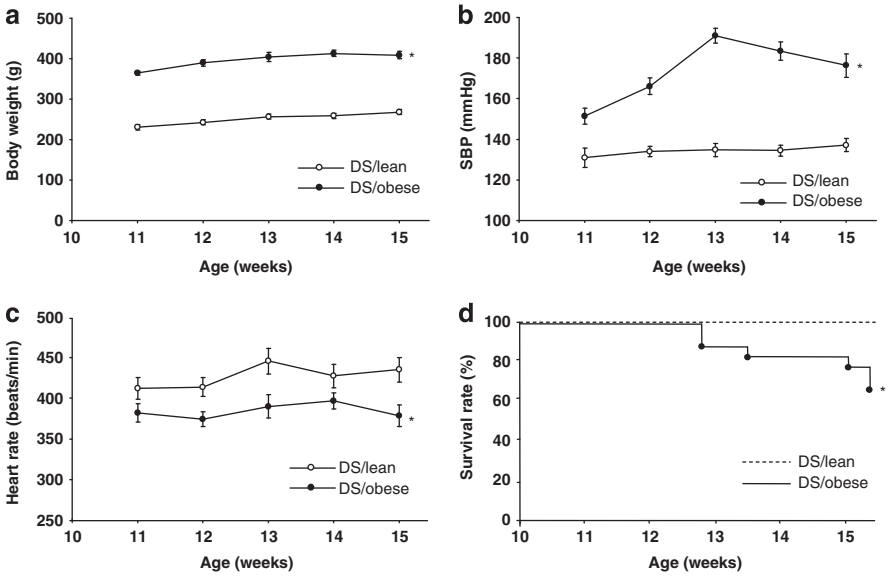

Figure 1 Time courses of physiological parameters as well as survival rate. Time courses of body weight (**a**), SBP (**b**), and heart rate (**c**) as well as Kaplan–Meier plots of survival rate (**d**) for DS/lean and DS/obese rats. Data for body weight, SBP and heart rate are means ± s.e.m. for surviving animals ($n=10$ and 21 at 11 weeks and $n=10$ and 14 at 15 weeks for DS/lean and DS/obese rats, respectively). *$P<0.05$ *vs.* DS/lean rats.

Echocardiography revealed that in both male and female genders, IVST, LVPWT and RWT were significantly greater in DS/obese rats than in DS/lean rats (Table 2, Supplementary Table 3 in Supplementary Material online). Both LVFS and LV ejection fraction were also increased in DS/obese rats compared with DS/lean rats in both genders. The *E*/*A* ratio was significantly decreased and both deceleration time and IRT, which are indices of LV relaxation, were significantly increased in DS/obese rats compared with DS/lean rats in both genders. The Tei index, an overall index of LV contraction and relaxation, was also significantly increased in DS/obese rats in both genders. There were no significant differences in parameters LV systolic and diastolic function between male and female animals of the same genotype. These results thus indicated that LV diastolic function was impaired in DS/obese rats in both genders.

Table 2 Echocardiographic parameters of DS/lean and DS/obese rats at 15 weeks of age

Parameter	*DS/lean*	*DS/obese*
Heart rate (beats per min)	215 ± 4	206 ± 16
IVST (mm)	1.80 ± 0.08	2.38 ± 0.03*
LVPWT (mm)	1.79 ± 0.06	2.32 ± 0.04*
LVDd (mm)	6.56 ± 0.08	6.94 ± 0.21
LVDs (mm)	3.09 ± 0.15	2.64 ± 0.13
LVFS (%)	53.6 ± 2.4	64.7 ± 1.6*
LVEF (%)	81.7 ± 1.9	90.9 ± 1.0*
LV mass (mg)	742 ± 32	1447 ± 42*
RWT	0.53 ± 0.02	0.64 ± 0.02*
E/*A*	1.97 ± 0.07	1.49 ± 0.05*
DcT (ms)	42.8 ± 2.5	52.9 ± 1.9*
IRT (ms)	19.0 ± 1.3	35.4 ± 2.1*
Tei index	0.37 ± 0.02	0.45 ± 0.02*

Abbreviations: Dct, deceleration time; DS, Dahl salt-sensitive; IRT, isovolumic relaxation time; IVST, interventricular septum thickness; LV mass, left ventricular mass; LVDd, LV end-diastolic; LVDs, LV end-systolic; LVEF, LV ejection fraction; LVFS, LV fractional shortening; LVPWT, LV posterior wall thickness; RWT, relative wall thickness.
*$P<0.05$ *vs.* DS/lean rats.
Data are means ± s.e.m. for surviving animals ($n=10$ and 14 for DS/lean rats and DS/obese rats, respectively).

Cardiomyocyte hypertrophy as well as cardiac fibrosis and gene expression

Microscopic analysis revealed that the cross-sectional area of cardiac myocytes in DS/obese rats was increased compared with that in DS/lean rats (Figures 2a and b). Hemodynamic overload was also associated with marked upregulation of the expression of fetal-type cardiac genes, including those for atrial natriuretic peptide, brain natriuretic peptide and β-myosin heavy chain, in the left ventricle of DS/obese rats (Figures 2c–e).

Azan–Mallory staining revealed that fibrosis in perivascular and interstitial regions of the LV myocardium was increased in DS/obese rats compared with DS/lean rats (Figures 3a–c). The abundance of mRNAs for collagen types I and III in the heart of DS/obese rats was also increased compared with that in DS/lean rats (Figures 3d and e). In addition, the amounts of TGF-β1 and CTGF mRNAs, which correlate with cardiac fibrosis and growth, were increased in DS/obese rats compared with DS/lean rats (Figures 3f and g).

Cardiac oxidative stress

Superoxide production in myocardial tissue sections revealed by staining with dihydroethidium as well as the activity of NADPH oxidase in LV homogenates were both increased in DS/obese rats compared with DS/lean rats (Figures 4a–c). The expression of genes for the $p22^{phox}$ and $gp91^{phox}$ membrane components and for the $p47^{phox}$ $p67^{phox}$ and Rac1 cytoplasmic components of NADPH oxidase in the heart was also upregulated in DS/obese rats compared with DS/lean rats (Figures 4d–h).

Cardiac inflammation

Immunostaining for the monocyte–macrophage marker CD68 revealed that macrophage infiltration in the LV myocardium was increased in DS/obese rats compared with DS/lean rats (Figures 5a, b).

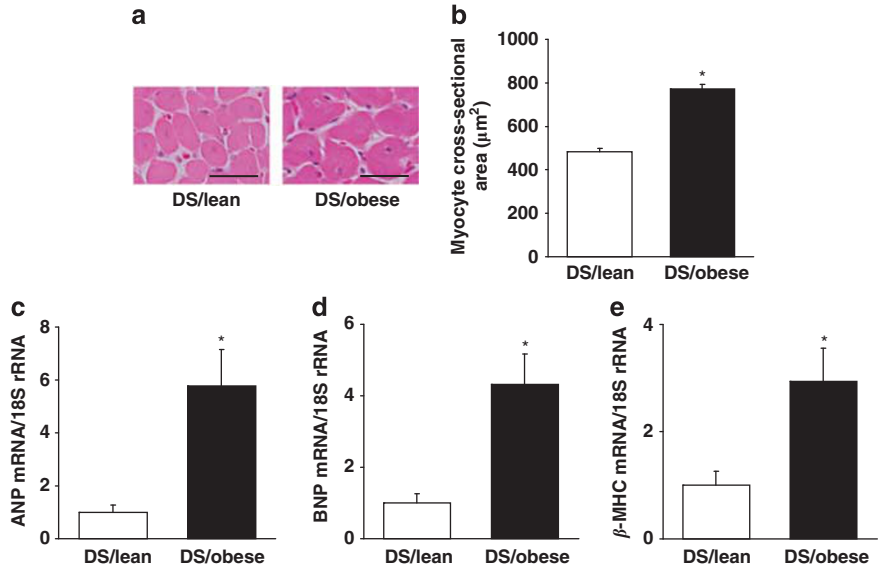

Figure 2 Cardiomyocyte size and expression of fetal-type cardiac genes. (**a**) Hematoxylin–eosin staining of transverse sections of the LV myocardium of DS/lean and DS/obese rats at 15 weeks of age. Scale bars, 50 μm. (**b**) Cross-sectional area of cardiac myocytes determined from sections similar to those in (**a**). (**c**–**e**) Quantitative real-time (RT) PCR analysis of atrial natriuretic peptide (ANP), brain natriuretic peptide (BNP), and β-myosin heavy chain (β-MHC) mRNAs in the left ventricle of DS/lean and DS/obese rats at 15 weeks of age, respectively. The amount of each mRNA was normalized by that of 18S rRNA and then expressed relative to the mean value for DS/lean rats. Data in (**b**) through (**e**) are means ± s.e.m. for surviving animals ($n=10$ and 14 for DS/lean and DS/obese rats, respectively). *$P<0.05$ *vs.* DS/lean rats.

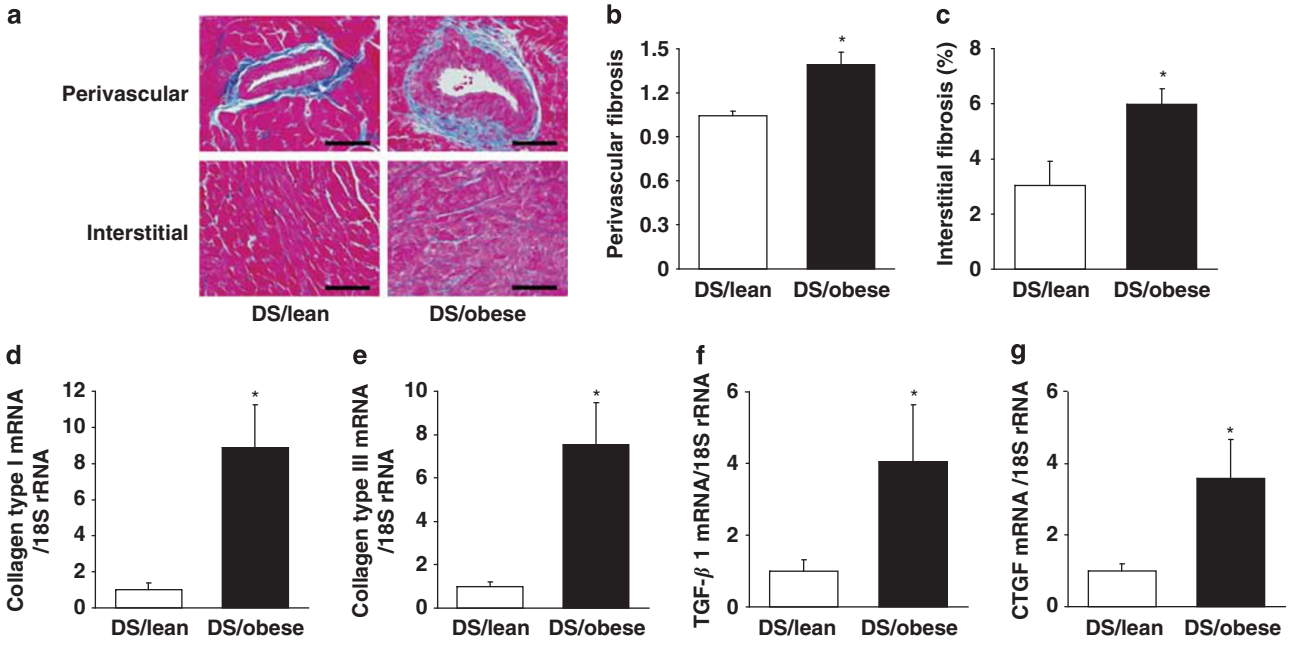

Figure 3 Cardiac fibrosis and gene expression. (**a**) Collagen deposition as revealed by Azan–Mallory staining in perivascular (upper panels) or interstitial (lower panels) regions of the LV myocardium of DS/lean and DS/obese rats at 15 weeks of age. Scale bars, 200 μm. (**b**, **c**) Relative extents of perivascular and interstitial fibrosis, respectively, in the LV myocardium as determined from sections similar to those in (**a**). (**d**–**g**) Quantitative real-time (RT) PCR analysis of collagen type I, collagen type III, TGF-β1, and CTGF mRNAs in the left ventricle of DS/lean and DS/obese rats at 15 weeks of age, respectively. The amount of each mRNA was normalized by that of 18S rRNA and then expressed relative to the mean value for DS/lean rats. Data in (**b**) through (**g**) are means ± s.e.m. for surviving animals (n=10 and 14 for DS/lean and DS/obese rats, respectively). *P<0.05 *vs.* DS/lean rats.

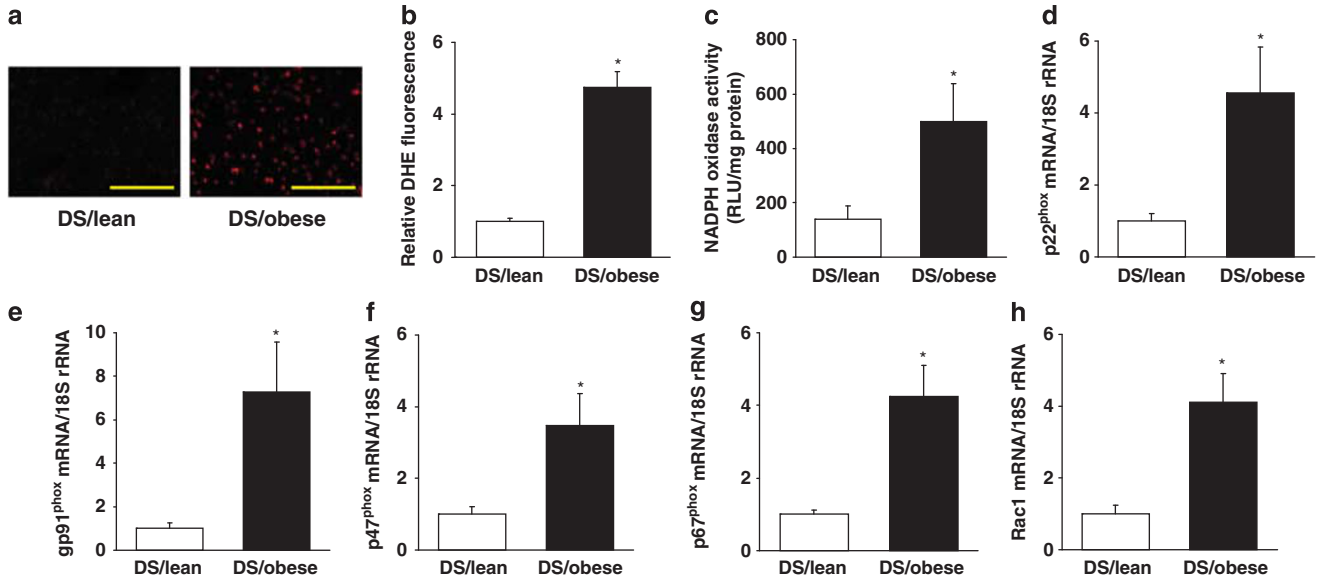

Figure 4 Superoxide production and nicotinamide adenine dinucleotide phosphate (NADPH) oxidase activity as well as expression of NADPH oxidase subunit genes. (**a**) Superoxide production as revealed by dihydroethidium staining in interstitial regions of the LV myocardium of DS/lean and DS/obese rats at 15 weeks of age. Scale bars, 100 μm. (**b**) Dihydroethidium fluorescence intensity determined from sections similar to those in (**a**). Data are expressed as the relative differences compared with DS/lean rats. (**c**) NADPH-dependent superoxide production in LV homogenates of DS/lean and DS/obese rats at 15 weeks of age. Results are expressed as relative light units (RLU) per mg of protein. (**d**–**h**) Quantitative real-time (RT) PCR analysis of $p22^{phox}$, $gp91^{phox}$, $p47^{phox}$, $p67^{phox}$ and Rac1 mRNAs in the left ventricle of DS/lean and DS/obese rats at 15 weeks of age, respectively. The amount of each mRNA was normalized by that of 18S rRNA and then expressed relative to the mean value for DS/lean rats. Data in (**b**) through (**h**) are means ± s.e.m. for surviving animals (n=10 and 14 for DS/lean and DS/obese rats, respectively). *P<0.05 *vs.* DS/lean rats.

The expression of monocyte chemoattractant protein-1, TNF-α and IL-6 genes in the left ventricle was also increased in DS/obese rats compared with DS/lean rats (Figures 5c–e).

Activity of the RAAS

DS/obese rats showed a decrease in both renin activity and Ang II concentration in plasma, as well as an increase in the ratio of serum

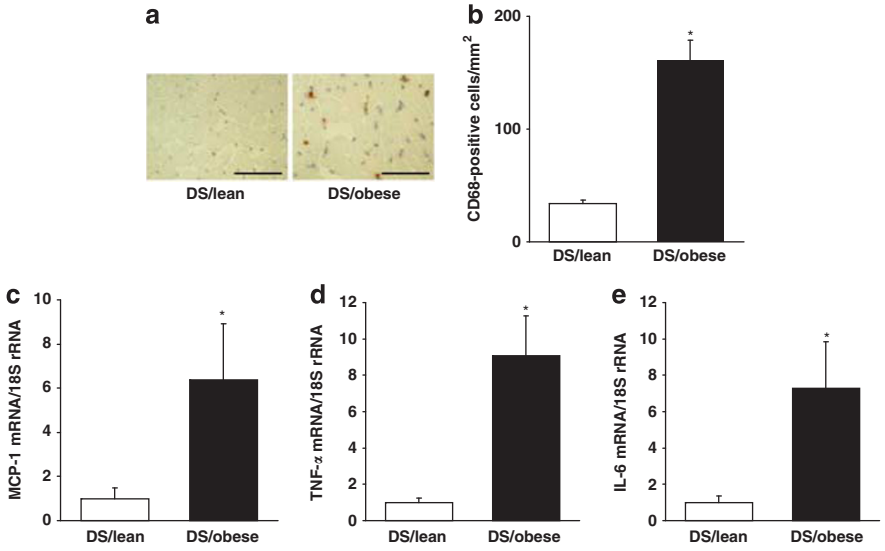

Figure 5 Macrophage infiltration and cytokine gene expression. (**a**) Immunohistochemical analysis of the monocyte–macrophage marker CD68 of the LV myocardium of DS/lean and DS/obese rats at 15 weeks of age. Scale bars, 50 μm. (**b**) Density of CD68-positive cells determined from sections similar to those in (**a**). (**c**–**e**) Quantitative real-time (RT) PCR analysis of monocyte chemoattractant protein-1 (MCP-1), TNF-α and IL-6 mRNAs in the left ventricle of DS/lean and DS/obese rats at 15 weeks of age, respectively. The amount of each mRNA was normalized by that of 18S rRNA and then expressed relative to the mean value for DS/lean rats. Data in (**b**) through (**e**) are means ± s.e.m. for surviving animals (n=10 and 14 for DS/lean and DS/obese rats, respectively). *$P<0.05$ *vs.* DS/lean rats.

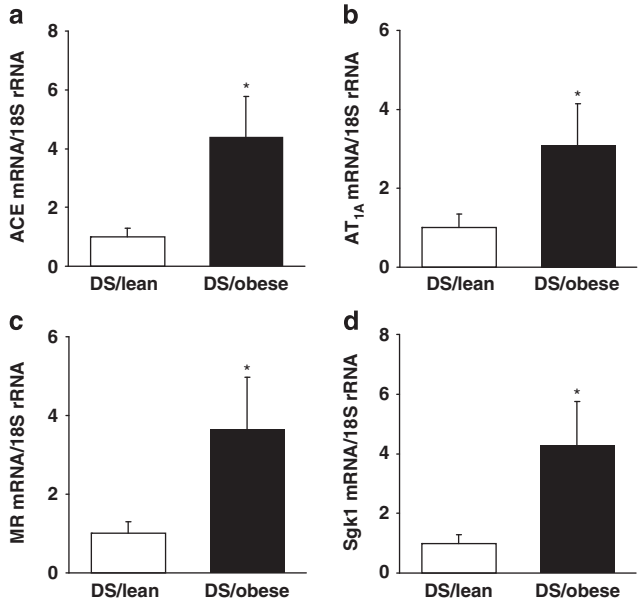

Figure 6 Expression of angiotensin-converting enzyme (ACE), Ang II type 1A receptor (AT_{1A}), MR and serum/glucocorticoid-regulated kinase 1 (Sgk1) genes. Quantitative real-time (RT) PCR analysis of mRNAs for ACE (**a**), AT_{1A} (**b**), MR (**c**), and Sgk1 (**d**) in the left ventricle of DS/lean and DS/obese rats at 15 weeks of age. The amount of each mRNA was normalized by that of 18S rRNA and then expressed relative to the mean value for DS/lean rats. Data are means ± s.e.m. for surviving animals (n=10 and 14 for DS/lean and DS/obese rats, respectively). *$P<0.05$ *vs.* DS/lean rats.

aldosterone concentration to plasma renin activity compared with DS/lean rats (Table 1). The serum aldosterone concentration did not differ significantly between the two strains. Finally, the expression of angiotensin-converting enzyme, Ang II type 1A receptor, MR and serum/glucocorticoid-regulated kinase 1 genes in the left ventricle was increased in DS/obese rats compared with DS/lean rats (Figure 6).

DISCUSSION

We have now found that female DS/obese rats fed a normal diet develop obesity as well as salt-sensitive hypertension, dyslipidemia and type 2 diabetes mellitus including insulin resistance, suggesting that female DS/obese rats may be a good animal model of human MetS as we previously shown for DS/obese males.[9] In addition, female DS/obese rats developed LV hypertrophy, fibrosis and diastolic dysfunction as well as cardiac oxidative stress and inflammation. Both low-renin hypertension with relative aldosterone excess and activation of the cardiac RAAS may have contributed to cardiac remodeling and diastolic dysfunction in these animals.

Blood pressure in genetically obese animals with leptin resistance, including Zucker fatty (*fa/fa*) rats, has been shown to be reduced or at least not elevated compared with that in corresponding lean littermates.[24] In the present study, however, SBP was higher in DS/obese rats than in DS/lean rats and in Zucker fatty rats at 11 weeks and thereafter, suggesting that the presence of the *fa* allele of *Lepr* on the DahlS background is associated with increased salt sensitivity of blood pressure, which may contribute to the development of cardiovascular complications and premature death within shorter period than in Zucker fatty rats.[9,25] The arterial pressure control mechanism of diuresis and natriuresis appears to be shifted toward higher blood pressure levels in obese individuals.[26] The elevation of SBP in DS/obese rats was also accompanied by the increases in both homeostasis model assessment–insulin resistance and cardiac inflammatory responses, consistent with the concept that insulin resistance and inflammation may give rise to an altered profile of vascular function and thereby lead to hypertension.[26]

Obesity, especially when complicated with hypertension, is associated with changes in cardiac structure and function.[27] Concentric cardiac remodeling was the most prevalent pattern noted in obese subjects, with concentric hypertrophy being the most prevalent in obese subjects with hypertension. Furthermore, obesity, hypertension and concentric hypertrophy were found to be independent predictors of diastolic dysfunction. Given that both the ratio of LV weight to

tibial length (or echocardiography-derived LV mass) and the RWT, as well as the expression of fetal-type cardiac genes were significantly increased in female DS/obese rats, concentric LV hypertrophy was also induced in association with obesity and hypertension in these animals. Cardiac fibrosis is a pathological feature associated with hypertension and is responsible for LV diastolic dysfunction, likely as a result of increased LV diastolic stiffness.[18] DS/obese rats developed hypertension and showed impairment of LV relaxation as well as an increase in the extents of LV perivascular and interstitial fibrosis, and these changes were accompanied by upregulation of TGF-β1 and CTGF mRNAs in the heart, consistent with previous observations showing that these growth factors are involved in the development of LV remodeling in a rat model of heart failure[28] and in SHR/NDmcr-cp rats fed a high-salt diet.[8]

Macrophages have been implicated in fibrosis associated with various pathological conditions. In the present study, macrophage infiltration into the interstitial space of the myocardium was accompanied by upregulation of the expression of genes for proinflammatory chemokines and cytokines, including those for monocyte chemoattractant protein-1, TNF-α and IL-6, in the heart of DS/obese rats. These changes may thus have contributed to myocardial fibrosis.[29] monocyte chemoattractant protein-1 has an important role in the infiltration of inflammatory cells into cardiovascular tissue and has been associated with the progression and severity of heart failure in rats.[18] TNF-α is a proimflammatory cytokine that has been implicated in the pathogenesis of cardiovascular diseases such as acute myocardial infarction, chronic heart failure and atherosclerosis, and cardiac overexpression of TNF-α causes LV remodeling.[30] IL-6 is secreted by cardiomyocyte and increased in failing hearts.[31] The increased IL-6 is involved in diabetic deterioration and may be associated with cardiac hypertrophy.[32]

Increased oxidative stress has been recognized in experimental animal and human obesity, and may contribute to the development of MetS.[33] Experimental models of heart failure also support the notion that increased oxidative stress has a role in the pathogenesis of myocardial remodeling and failure.[34] We found that both NADPH-dependent superoxide generation and the expression of NADPH oxidase subunit genes were increased in the heart of DS/obese rats, consistent with data from SHR/NDmcr-cp rats.[8] Excess reactive oxygen species may contribute to impairment of LV diastolic function through inhibition of Ca^{2+}-handling proteins.[35] In addition to impairments in metabolic signaling and oxidative stress, genetic and environmental factors, aging and hyperglycemia all contribute to reduced mitochondrial biogenesis and mitochondrial dysfunction.[4] These mitochondrial abnormalities can predispose a metabolic cardiomyopathy characterized by diastolic dysfunction. Reactive oxygen species (ROS) generated by dysfunctional mitochondria may have contributed to myocardial oxidative stress in DS/obese rats. In failing myocardium, there is increased expression of TNF-α.[36] Increases in TNF-α expression induce activation of NADPH oxidase and production of ROS.[37] Increased myocardial IL-6 expression is associated with the progression of heart failure.[38] IL-6 is produced by myocardium in heart disease and might be stimulated by ROS.[39] IL-6 also increases the formation of ROS.[40] These observations suggest that oxidative stress induced by these inflammatory cytokines may have a role in cardiac remodeling and diastolic dysfunction in DS/obese rats.

The RAAS has also been implicated in the pathogenesis of MetS.[41] Individuals with low-renin or salt-sensitive hypertension have an increased risk of end organ damage, cardiovascular events and mortality compared with those with other types of hypertension.[42] Patients with low-renin hypertension and relative aldosterone excess have impaired endothelial function, which might contribute to adverse outcomes.[43] In the present study, renin activity and the concentration of Ang II in plasma were markedly reduced in DS/obese rats compared with DS/lean rats, whereas the serum aldosterone concentration did not differ between the two strains, similar to hormonal data from obese hypertensive women in comparison with obese normotensive women.[44] These findings are indicative of inappropriate aldosterone secretion, possibly as a result of an increased adrenocortical sensitivity to Ang II. Treatment of adrenocortical cells with LDL was previously shown to result in marked potentiation of the Ang II-induced production of aldosterone.[44] The increase in the aldosterone/renin ratio observed in DS/obese rats may thus be attributable to the elevated LDL level or to other adipocyte-derived aldosterone-releasing factors.[45] Whereas the systemic renin–angiotensin system was suppressed, we found that the expression of angiotensin-converting enzyme and Ang II type 1A receptor genes was increased in the heart of DS/obese rats, consistent with previous data showing that the cardiac renin–angiotensin system was activated in response to pressure overload in rats with salt-sensitive hypertension.[10,18] Aldosterone and the MR have also been recently implicated in the development of MetS.[46] Whereas the serum aldosterone concentration was not altered in DS/obese rats, the abundance of mRNAs for the MR and the aldosterone effector kinase serum/glucocorticoid-regulated kinase 1 was increased in the heart, consistent with a pathological role for ligand-independent MR activation.[47] Relative aldosterone excess in the setting of low-renin activity and enhanced MR signaling in the myocardium results in increased oxidative stress and inflammation, leading to the development of cardiac remodeling and dysfunction.[18,48] These data are also consistent with previous results showing that serum/glucocorticoid-regulated kinase 1 enhances myocardial hypertrophic response as well as has a role in mineralocorticoid-induced tissue fibrosis.[49,50] Together, these observations suggest that relative aldosterone excess and activation of the cardiac RAAS may be involved in the pathogenesis of LV remodeling and diastolic dysfunction in DS/obese rats.

We used female DS/obese and DS/lean rats because this study aimed to investigate whether the phenotype of female DS/obese rats is similar to that of male DS/obese rats, which have recently been characterized as a new animal model of MetS.[9] As a result, the cardiac phenotype in female DS/obese rats has been found to be qualitatively similar to that of male DS/obese rats.

In conclusion, the phenotype of female DS/obese rats fed a normal diet is consistent with that of MetS in humans. Both male and female DS/obese rats may thus be an appropriate model for this condition. These animals develop salt-sensitive hypertension as well as LV diastolic dysfunction, hypertrophy and fibrosis, all of which are accompanied by increased cardiac oxidative stress and inflammation. Relative aldosterone excess and activation of the cardiac RAAS may contribute to the pathogenesis of cardiac remodeling and diastolic dysfunction in these animals. Further investigations are required to clarify the molecular mechanisms that underlie MetS and its associated cardiac injury.

CONFLICT OF INTEREST

The authors declare no conflict of interest.

ACKNOWLEDGEMENTS

We thank Mayuko Furukawa, Koji Tsuboi, Yuichiro Yamada, Chisa Inoue, Tomomi Inoue, Haruka Tsukamoto, Masafumi Sakai and Chieko Nakashima for technical assistance. This work was supported by unrestricted research grants from the Mitsubishi Tanabe Pharma Corp. (Osaka, Japan) and Kyowa Hakko Kirin Co Ltd (Tokyo, Japan) as well as by Management Expenses Grants from the Japanese government to Nagoya University.

1 Dandona P, Aljada A, Chaudhuri A, Mohanty P, Garg R. Metabolic syndrome: a comprehensive perspective based on interactions between obesity, diabetes, and inflammation. *Circulation* 2005; **111**: 1448–1454.
2 Matsuzawa Y, Funahashi T, Nakamura T. Molecular mechanism of metabolic syndrome X: contribution of adipocytokines adipocyte-derived bioactive substances. *Ann NY Acad Sci* 1999; **892**: 146–154.
3 Mathieu P, Poirier P, Pibarot P, Lemieux I, Despres JP. Visceral obesity: the link among inflammation, hypertension, and cardiovascular disease. *Hypertension* 2009; **53**: 577–584.
4 Ren J, Pulakat L, Whaley-Connell A, Sowers JR. Mitochondrial biogenesis in the metabolic syndrome and cardiovascular disease. *J Mol Med* 2010; **88**: 993–1001.
5 Wong CY, O'Moore-Sullivan T, Fang ZY, Haluska B, Leano R, Marwick TH. Myocardial and vascular dysfunction and exercise capacity in the metabolic syndrome. *Am J Cardiol* 2005; **96**: 1686–1691.
6 Grandi AM, Maresca AM, Giudici E, Laurita E, Marchesi C, Solbiati F, Nicolini E, Guasti L, Venco A. Metabolic syndrome and morphofunctional characteristics of the left ventricle in clinically hypertensive nondiabetic subjects. *Am J Hypertens* 2006; **19**: 199–205.
7 Carroll JF, Zenebe WJ, Strange TB. Cardiovascular function in a rat model of diet-induced obesity. *Hypertension* 2006; **48**: 65–72.
8 Matsui H, Ando K, Kawarazaki H, Nagae A, Fujita M, Shimosawa T, Nagase M, Fujita T. Salt excess causes left ventricular diastolic dysfunction in rats with metabolic disorder. *Hypertension* 2008; **52**: 287–294.
9 Hattori T, Murase T, Ohtake M, Inoue T, Tsukamoto H, Takatsu M, Kato Y, Hashimoto K, Murohara T, Nagata K. Characterization of a new animal model of metabolic syndrome: the DahlSZ-*Lepr*^{fa}/*Lepr*^{fa} rat. *Nutr Diab* 2011; **1**: e1; doi:10.1038/nutd.2010.1; published online 31 January 2011.
10 Nagata K, Somura F, Obata K, Odashima M, Izawa H, Ichihara S, Nagasaka T, Iwase M, Yamada Y, Nakashima N, Yokota M. AT1 receptor blockade reduces cardiac calcineurin activity in hypertensive rats. *Hypertension* 2002; **40**: 168–174.
11 Reffelmann T, Kloner RA. Transthoracic echocardiography in rats. Evalution of commonly used indices of left ventricular dimensions, contractile performance, and hypertrophy in a genetic model of hypertrophic heart failure (SHHF-Mcc-facp-Rats) in comparison with Wistar rats during aging. *Basic Res Cardiol* 2003; **98**: 275–284.
12 Sahn DJ, DeMaria A, Kisslo J, Weyman A. Recommendations regarding quantitation in M-mode echocardiography: results of a survey of echocardiographic measurements. *Circulation* 1978; **58**: 1072–1083.
13 Tei C, Ling LH, Hodge DO, Bailey KR, Oh JK, Rodeheffer RJ, Tajik AJ, Seward JB. New index of combined systolic and diastolic myocardial performance: a simple and reproducible measure of cardiac function—a study in normals and dilated cardiomyopathy. *J Cardiol* 1995; **26**: 357–366.
14 Wang CT, Navar LG, Mitchell KD. Proximal tubular fluid angiotensin II levels in angiotensin II-induced hypertensive rats. *J Hypertens* 2003; **21**: 353–360.
15 Mitchell KD, Bagatell SJ, Miller CS, Mouton CR, Seth DM, Mullins JJ. Genetic clamping of renin gene expression induces hypertension and elevation of intrarenal Ang II levels of graded severity in Cyp1a1-Ren2 transgenic rats. *J Renin Angiotensin Aldosterone Syst* 2006; **7**: 74–86.
16 Miyachi M, Yazawa H, Furukawa M, Tsuboi K, Ohtake M, Nishizawa T, Hashimoto K, Yokoi T, Kojima T, Murate T, Yokota M, Murohara T, Koike Y, Nagata K. Exercise training alters left ventricular geometry and attenuates heart failure in dahl salt-sensitive hypertensive rats. *Hypertension* 2009; **53**: 701–707.
17 Kato MF, Shibata R, Obata K, Miyachi M, Yazawa H, Tsuboi K, Yamada T, Nishizawa T, Noda A, Cheng XW, Murate T, Koike Y, Murohara T, Yokota M, Nagata K. Pioglitazone attenuates cardiac hypertrophy in rats with salt-sensitive hypertension: role of activation of AMP-activated protein kinase and inhibition of Akt. *J Hypertens* 2008; **26**: 1669–1676.
18 Nagata K, Obata K, Xu J, Ichihara S, Noda A, Kimata H, Kato T, Izawa H, Murohara T, Yokota M. Mineralocorticoid receptor antagonism attenuates cardiac hypertrophy and failure in low-aldosterone hypertensive rats. *Hypertension* 2006; **47**: 656–664.
19 Elmarakby AA, Loomis ED, Pollock JS, Pollock DM. NADPH oxidase inhibition attenuates oxidative stress but not hypertension produced by chronic ET-1. *Hypertension* 2005; **45**: 283–287.
20 Miyata K, Rahman M, Shokoji T, Nagai Y, Zhang GX, Sun GP, Kimura S, Yukimura T, Kiyomoto H, Kohno M, Abe Y, Nishiyama A. Aldosterone stimulates reactive oxygen species production through activation of NADPH oxidase in rat mesangial cells. *J Am Soc Nephrol* 2005; **16**: 2906–2912.
21 Somura F, Izawa H, Iwase M, Takeichi Y, Ishiki R, Nishizawa T, Noda A, Nagata K, Yamada Y, Yokota M. Reduced myocardial sarcoplasmic reticulum Ca(2+)-ATPase mRNA expression and biphasic force-frequency relations in patients with hypertrophic cardiomyopathy. *Circulation* 2001; **104**: 658–663.
22 Sakata Y, Yamamoto K, Mano T, Nishikawa N, Yoshida J, Hori M, Miwa T, Masuyama T. Activation of matrix metalloproteinases precedes left ventricular remodeling in hypertensive heart failure rats: its inhibition as a primary effect of Angiotensin-converting enzyme inhibitor. *Circulation* 2004; **109**: 2143–2149.
23 Yamada T, Nagata K, Cheng XW, Obata K, Saka M, Miyachi M, Naruse K, Nishizawa T, Noda A, Izawa H, Kuzuya M, Okumura K, Murohara T, Yokota M. Long-term administration of nifedipine attenuates cardiac remodeling and diastolic heart failure in hypertensive rats. *Eur J Pharmacol* 2009; **615**: 163–170.
24 Verma S, Leung YM, Yao L, Battell M, Dumont AS, McNeill JH. Hyperinsulinemia superimposed on insulin resistance does not elevate blood pressure. *Am J Hypertens* 2001; **14**: 429–432.
25 Johnson PR, Stern JS, Horwitz BA, Harris Jr RE, Greene SF. Longevity in obese and lean male and female rats of the Zucker strain: prevention of hyperphagia. *Am J Clin Nutr* 1997; **66**: 890–903.
26 Kotsis V, Stabouli S, Papakatsika S, Rizos Z, Parati G. Mechanisms of obesity-induced hypertension. *Hypertens Res* 2010; **33**: 386–393.
27 Dhuper S, Abdullah RA, Weichbrod L, Mahdi E, Cohen HW. Association of Obesity and Hypertension With Left Ventricular Geometry and Function in Children and Adolescents. *Obesity (Silver Spring)* 2010; **19**: 128–133; e-pub ahead of print 17 June 2010.
28 Ahmed MS, Oie E, Vinge LE, Yndestad A, Oystein Andersen G, Andersson Y, Attramadal T, Attramadal H. Connective tissue growth factor—a novel mediator of angiotensin II-stimulated cardiac fibroblast activation in heart failure in rats. *J Mol Cell Cardiol* 2004; **36**: 393–404.
29 Kuwahara F, Kai H, Tokuda K, Takeya M, Takeshita A, Egashira K, Imaizumi T. Hypertensive myocardial fibrosis and diastolic dysfunction: another model of inflammation? *Hypertension* 2004; **43**: 739–745.
30 Meldrum DR, Cleveland Jr JC, Cain BS, Meng X, Harken AH. Increased myocardial tumor necrosis factor-alpha in a crystalloid-perfused model of cardiac ischemia-reperfusion injury. *Ann Thorac Surg* 1998; **65**: 439–443.
31 Hogye M, Mandi Y, Csanady M, Sepp R, Buzas K. Comparison of circulating levels of interleukin-6 and tumor necrosis factor-alpha in hypertrophic cardiomyopathy and in idiopathic dilated cardiomyopathy. *Am J Cardiol* 2004; **94**: 249–251.
32 Jialal I, Devaraj S, Venugopal SK. Oxidative stress, inflammation, and diabetic vasculopathies: the role of alpha tocopherol therapy. *Free Radic Res* 2002; **36**: 1331–1336.
33 Furukawa S, Fujita T, Shimabukuro M, Iwaki M, Yamada Y, Nakajima Y, Nakayama O, Makishima M, Matsuda M, Shimomura I. Increased oxidative stress in obesity and its impact on metabolic syndrome. *J Clin Invest* 2004; **114**: 1752–1761.
34 Sawyer DB, Siwik DA, Xiao L, Pimentel DR, Singh K, Colucci WS. Role of oxidative stress in myocardial hypertrophy and failure. *J Mol Cell Cardiol* 2002; **34**: 379–388.
35 Adachi T, Weisbrod RM, Pimentel DR, Ying J, Sharov VS, Schoneich C, Cohen RA. S-Glutathiolation by peroxynitrite activates SERCA during arterial relaxation by nitric oxide. *Nat Med* 2004; **10**: 1200–1207.
36 El-Menyar AA. Cytokines and myocardial dysfunction: state of the art. *J Card Fail* 2008; **14**: 61–74.
37 Gao X, Belmadani S, Picchi A, Xu X, Potter BJ, Tewari-Singh N, Capobianco S, Chilian WM, Zhang C. Tumor necrosis factor-alpha induces endothelial dysfunction in Lepr(db) mice. *Circulation* 2007; **115**: 245–254.
38 Plenz G, Song ZF, Reichenberg S, Tjan TD, Robenek H, Deng MC. Left-ventricular expression of interleukin-6 messenger-RNA higher in idiopathic dilated than in ischemic cardiomyopathy. *Thorac Cardiovasc Surg* 1998; **46**: 213–216.
39 Newman WH, Castresana MR, Webb JG, Detmer K, Wang Z. Isoproterenol inhibits transcription of cardiac cytokine genes induced by reactive oxygen intermediates. *Anesthesiology* 2002; **96**: 947–954.
40 Srivastava S, Vladykovskaya EN, Haberzettl P, Sithu SD, D'Souza SE, States JC. Arsenic exacerbates atherosclerotic lesion formation and inflammation in ApoE$^{-/-}$ mice. *Toxicol Appl Pharmacol* 2009; **241**: 90–100.
41 Boustany CM, Bharadwaj K, Daugherty A, Brown DR, Randall DC, Cassis LA. Activation of the systemic and adipose renin-angiotensin system in rats with diet-induced obesity and hypertension. *Am J Physiol Regul Integr Comp Physiol* 2004; **287**: R943–R949.
42 Morimoto A, Uzu T, Fujii T, Nishimura M, Kuroda S, Nakamura S, Inenaga T, Kimura G. Sodium sensitivity and cardiovascular events in patients with essential hypertension. *Lancet* 1997; **350**: 1734–1737.
43 Duffy SJ, Biegelsen ES, Eberhardt RT, Kahn DF, Kingwell BA, Vita JA. Low-renin hypertension with relative aldosterone excess is associated with impaired NO-mediated vasodilation. *Hypertension* 2005; **46**: 707–713.
44 Lamounier-Zepter V, Rotthoff T, Ansurudeen I, Kopprasch S, Scherbaum WA, Ehrhart-Bornstein M, Bornstein SR. Increased aldosterone/renin quotient in obese hypertensive women: a novel role for low-density lipoproteins? *Horm Metab Res* 2006; **38**: 471–475.
45 Fujita T. Mineralocorticoid receptors, salt-sensitive hypertension, and metabolic syndrome. *Hypertension* 2010; **55**: 813–818.
46 Nagase M, Fujita T. Mineralocorticoid receptor activation in obesity hypertension. *Hypertens Res* 2009; **32**: 649–657.
47 Shibata S, Nagase M, Yoshida S, Kawarazaki W, Kurihara H, Tanaka H, Miyoshi J, Takai Y, Fujita T. Modification of mineralocorticoid receptor function by Rac1 GTPase: implication in proteinuric kidney disease. *Nat Med* 2008; **14**: 1370–1376.
48 Nagata K. Mineralocorticoid antagonism and cardiac hypertrophy. *Curr Hypertens Rep* 2008; **10**: 216–221.
49 Aoyama T, Matsui T, Novikov M, Park J, Hemmings B, Rosenzweig A. Serum and glucocorticoid-responsive kinase-1 regulates cardiomyocyte survival and hypertrophic response. *Circulation* 2005; **111**: 1652–1659.
50 Nagase M, Yoshida S, Shibata S, Nagase T, Gotoda T, Ando K, Fujita T. Enhanced aldosterone signaling in the early nephropathy of rats with metabolic syndrome: possible contribution of fat-derived factors. *J Am Soc Nephrol* 2006; **17**: 3438–3446.

Supplementary Information accompanies the paper on Hypertension Research website (http://www.nature.com/hr)